

Tomato HsfA1a plays a critical role in plant drought tolerance by activating *ATG* genes and inducing autophagy

Yu Wang,¹ Shuyu Cai,¹ Lingling Yin,¹ Kai Shi,^{1,2} Xiaojian Xia,^{1,2} Yanhong Zhou,^{1,2} Jingquan Yu,^{1,2,3} and Jie Zhou^{1,2,*}

¹Department of Horticulture; Zijingang Campus; Zhejiang University; Hangzhou, China; ²Zhejiang Provincial Key Laboratory of Horticultural Plant Integrative Biology; Hangzhou, China; ³Key Laboratory of Horticultural Plants Growth; Development and Quality Improvement; Agricultural Ministry of China; Hangzhou, China

Keywords: *ATG10*, *ATG18f*, autophagy, drought stress, *HsfA1a*, tomato, ubiquitination

Abbreviations: ABA, abscisic acid; ATG, autophagy-related; CDS, coding DNA sequence; ChIP, chromatin immunoprecipitation; EL, electrolyte leakage; EMSA, electrophoretic mobility shift assay; Hsf, heat-shock transcription factor; HSE, heat-shock element; Hsp, heat-shock protein; MDC, monodansylcadaverine; OE, overexpressing; PE, phosphatidylethanolamine; PTM, protein post-translational modification; RWC, relative water content; TEM, transmission electron microscopy; TF, transcription factor; TOR, target of rapamycin; TRV, tobacco rattle virus; Ub, ubiquitin; UPS, ubiquitin-26S proteasome system; VIGS, virus-induced gene silencing; WT, wild-type

Autophagy plays critical roles in plant responses to stress. In contrast to the wealth of information concerning the core process of plant autophagosome assembly, our understanding of the regulation of autophagy is limited. In this study, we demonstrated that transcription factor HsfA1a played a critical role in tomato tolerance to drought stress, in part through its positive role in induction of autophagy under drought stress. *HsfA1a* expression was induced by drought stress. Virus-induced *HsfA1a* gene silencing reduced while its overexpression increased plant drought tolerance based on both symptoms and membrane integrity. *HsfA1a*-silenced plants were more sensitive to endogenous ABA-mediated stomatal closure, while its overexpression lines were resistant under drought stress, indicating that phytohormone ABA did not play a major role in *HsfA1a*-induced drought tolerance. On the other hand, *HsfA1a*-silenced plants increased while its overexpression decreased the levels of insoluble proteins which were highly ubiquitinated under drought stress. Furthermore, drought stress induced numerous *ATGs* expression and autophagosome formation in wild-type plants. The expression of *ATG10* and *ATG18f*, and the formation of autophagosomes were compromised in *HsfA1a*-silenced plants but were enhanced in *HsfA1a*-overexpressing plants. Both electrophoretic mobility shift assay and chromatin immunoprecipitation coupled with qPCR analysis revealed that HsfA1a bound to *ATG10* and *ATG18f* gene promoters. Silencing of *ATG10* and *ATG18f* reduced HsfA1a-induced drought tolerance and autophagosome formation in plants overexpressing *HsfA1a*. These results demonstrate that HsfA1a induces drought tolerance by activating *ATG* genes and inducing autophagy, which may promote plant survival by degrading ubiquitinated protein aggregates under drought stress.

Introduction

Plants are often exposed to abiotic and biotic stresses (i.e. extreme temperatures, salt, drought, heavy metals, fungi and bacteria) that adversely affect their physiological traits, metabolic pathways, and protein activity. Repair or degradation of misfolded and damaged proteins, which are induced by stresses and are highly toxic to cell, relies on an elaborately regulated protein quality control system.¹ Molecular chaperones such as heat-shock proteins (Hsps) can promote folding and refolding of denatured proteins and the protein degradation systems such as autophagy

and the ubiquitin-26S proteasome system (UPS) to remove damaged and misfolded proteins.^{2,3} These processes are regulated by complex signaling networks including signaling molecules, protein kinases and transcription factors (TFs).⁴⁻⁶

Autophagy is an evolutionarily conserved protein degradation process in eukaryotes. The process is involved in the degradation of unnecessary or dysfunctional cellular components under environmental stress conditions or during certain stages of development.⁷ During autophagy, cells create double-membrane-bound compartments called phagophores that engulf cytoplasmic components; the phagophore expands and seals to form a

© Yu Wang, Shuyu Cai, Lingling Yin, Kai Shi Xiaojian Xia, Yanhong Zhou, Jingquan Yu, and Jie Zhou

*Correspondence to: Jie Zhou; Email: jie@zju.edu.cn

Submitted: 05/06/2015; Revised: 09/05/2015; Accepted: 09/16/2015

<http://dx.doi.org/10.1080/15548627.2015.1098798>

This is an Open Access article distributed under the terms of the Creative Commons Attribution-Non-Commercial License (<http://creativecommons.org/licenses/by-nc/3.0/>), which permits unrestricted non-commercial use, distribution, and reproduction in any medium, provided the original work is properly cited. The moral rights of the named author(s) have been asserted.

double-membrane autophagosome. Then, the outer membrane of the autophagosome fuses with the tonoplast to release the internal vesicle as an autophagic body that will be recycled within the vacuole.⁸ More than 30 autophagy-related (*ATG*) genes, which encode core autophagic machineries and are the main genetic regulators of the autophagy process have been identified in plants over the last 20 years.^{9,10}

Although the critical roles of plant autophagy have been well established in a wide spectrum of biological processes, including stress responses, our understanding of the regulation and action mechanisms of plant autophagy is extremely limited. Most research on the mechanisms underlying autophagy regulation has traditionally focused on the TOR (target of rapamycin) kinase.¹¹ Silencing of the *TOR* gene in *Arabidopsis* leads to the constitutive formation of autophagosomes, indicating that TOR is a negative regulator of autophagy in plants.¹² Furthermore, a NADPH oxidase inhibitor blocks autophagy induction upon nutrient starvation and salt stress but not osmotic stress.¹³ Thus, ROS may mediate the induction of autophagy during some, but not all, stress conditions. We recently reported that silencing of the tomato *WRKY33* transcription factor genes compromise tomato heat tolerance and reduce heat-induced *ATG* gene expression and autophagosome accumulation, suggesting the possible involvement of tomato *WRKY33* in *ATG* induction.¹⁴ However, little information is available concerning the transcriptional regulation of plant autophagy genes under other stress conditions.

Heat-shock transcription factors (Hsfs) are a family of TFs found in all organisms that function as regulators of the genes encoding molecular chaperones and other stress proteins and enable survival following exposure to acute stress.¹⁵ Plants possess a uniquely complex Hsf family, with 21 members defined in *Arabidopsis thaliana*, 25 members in rice (*Oryza sativa*) and 24 members in tomato (*Solanum lycopersicum*).^{16,17} These Hsfs are classified into 3 conserved evolutionary categories (A, B and C) according to the structural features of their oligomerization domains.¹⁸ Class A Hsfs contain the transcriptional activation domain that is characterized by aromatic, large hydrophobic, and acidic amino acid residues. Class B and C Hsfs lack this particular amino acid motif and cannot induce transcriptional activation alone.^{18,19} There are 4 HsfA1 members in the class A1 group (HsfA1a, HsfA1b, HsfA1c and HsfA1e).^{20,21} HsfA1a is a master regulator that functions both as an activator and as a repressor of its target genes under heat-shock stress.^{22,23} Exposure to heat stress leads to oligomerization of HsfA1a into active trimers, followed by its translocation into the nucleus and binding to the heat-shock elements (HSEs) located within the promoter regions of target genes (i.e., *HsfA2*, *Hsp70*, and *Hsp90*).²⁴ HsfA1a can also interact with the HsfA2, Hsp70, and Hsp90 proteins to form a heterooligomeric complex that exhibits a versatile ability to regulate the plant stress response.^{24,25} Transgenic *Arabidopsis* and tomato plants overexpressing HsfA1a proteins show constitutive heat-shock protein synthesis and exhibit enhanced basic thermotolerance.^{26,27} In addition to heat stress, HsfA1a also mediates plant tolerance to salt, drought and oxidative stresses by inducing genes encoding Hsp proteins.^{22,24} However, the functions of HsfA1a in the regulation of the expression of non-heat-

shock responsive genes under stress conditions are less well understood.

To better understand the mechanistic basis of autophagy regulation in plant stress responses, we sought to identify and functionally analyze the involvement of HsfA1a in autophagy under drought stress. Gene overexpression and tobacco rattle virus (TRV)-induced gene silencing (VIGS) have been extensively used for functional gene analysis in plants including *Arabidopsis*,²⁸ *Nicotiana* species²⁹ and tomato,³⁰ despite their potential complications associated with high levels of transgene products and viral infection, which can be largely overcome by using appropriate controls. We showed that HsfA1a, a transcription factor with a broad role in plant abiotic stress responses, was a positive regulator of drought-induced autophagy. Using an electrophoretic mobility shift assay (EMSA) and chromatin immunoprecipitation coupled with qPCR (ChIP-qPCR) analysis, we revealed that HsfA1a directly bound to the promoters of 2 autophagy genes (*ATG10* and *ATG18f*). Silencing these 2 autophagy genes compromised HsfA1a-mediated plant drought tolerance and autophagosome production. This is the first study to demonstrate that the multifunctional transcription factor HsfA1a is responsive to drought treatment and plays a positive role in induction of the *ATG10* and *ATG18f* genes and the formation of autophagosomes under drought stress. HsfA1a acts as a positive regulator in autophagy-induced drought tolerance in the tomato plants.

Results

Induction of the *HsfA1a* gene and the phenotypes of plants with silenced or overexpressed *HsfA1a* under drought stress

To analyze the possible involvement of HsfA1a in plant dehydration tolerance, we first examined the expression pattern of *HsfA1a* in response to drought stress. As shown in **Fig. 1A**, the transcript level of the *HsfA1a* gene remained largely constant throughout the 13-day experimental period under normal water supply conditions. However, when water was withheld, the *HsfA1a* transcript level was increased by as early as the 3rd day and remained elevated up to 13 d under dehydration stress (**Fig. 1A**). Notably, the largest increase in the *HsfA1a* transcript level was observed after 6 d under drought stress, when the plants began to show symptoms of dehydration (**Fig. 1A**).

To directly analyze the role of HsfA1a in drought tolerance, we compared WT and F2 progeny of *HsfA1a*-overexpressing (*HsfA1a*OE) plants from 2 independent lines (1# and 3#) expressing high HsfA1a protein levels (**Fig. S1**). We also analyzed *HsfA1a*-silenced (TRV-*HsfA1a*) plants, which had only 30 to 40% of *HsfA1a* transcript levels of the TRV control plants (**Fig. S2**). The transcript levels of other 3 *HsfA1* homologous genes (*HsfA1b*, *HsfA1c* and *HsfA1e*) were not changed in the TRV-*HsfA1a* plants when compared to those of the TRV control plants (**Fig. S2**). Only some margins of old leaves displayed symptoms of dehydration after withholding water for 13 d in the drought-treated TRV and WT plants, whereas a majority of the leaves remained green (**Fig. 1B and C**). In contrast, a majority of the leaves from TRV-*HsfA1a* plants exhibited extensive wilting after 13 d under drought stress (**Fig. 1B**). The relative water

content (RWC) was similar in all the plants under normal water supply (Fig. 1D). However, the RWC of TRV-*HsfA1a* plants was 36.4% less than that of TRV plants under drought stress (Fig. 1D). The RWC of *HsfA1a*OE-1# and *HsfA1a*OE-3# was 24.7% and 29.4%, respectively, higher than that of WT plants after 13 d under drought stress (Fig. 1D). Furthermore, the electrolyte leakage (EL) value of TRV-*HsfA1a* plants was similar to that of TRV plants when they were grown with a normal water supply. However, the EL value of TRV-*HsfA1a* plants was 58.7% higher than the TRV plants after 13 d of drought stress (Fig. S3). Drought tolerance was significantly increased in both lines of *HsfA1a*OE plants, and the EL values of *HsfA1a*OE-1# and *HsfA1a*OE-3# were reduced by 47.1% and 53.3%, respectively, when compared with those of the WT plants after 13 d under drought stress (Fig. 1C and Fig. S3). Thus, the membrane integrity was more sensitive in TRV-*HsfA1a* plants than that of TRV plants. By contrast, the membrane integrity of plants overexpressing *HsfA1a* was more resistant than that of the WT plants under drought stress.

Association of drought sensitivity or tolerance and the protein-ubiquitin conjugates in *HsfA1a*-silenced or -overexpressing plants under drought stress

Drought is known to induce plant stomatal closure and abscisic acid (ABA) accumulation. To determine whether *HsfA1a* was involved in stomatal closure and ABA accumulation under drought stress, we silenced the *HsfA1a* gene and overexpression of *HsfA1a* in tomato plants and analyzed the stomatal aperture and ABA content. As shown in Fig. 2, the stomata were open in TRV, TRV-*HsfA1a*, WT and *HsfA1a*OE plants, and the ratio of stomatal aperture length over width (which indicates the degree of stomatal closure) and ABA content were similar under normal water conditions. However, the stomata of TRV plants were closed and the ratio of stomatal aperture length over width and ABA accumulation were significantly increased after 6 d under drought stress (84.6% and 137.6%, respectively; Fig. 2B and C). Interestingly, the stomatal closure was more pronounced in

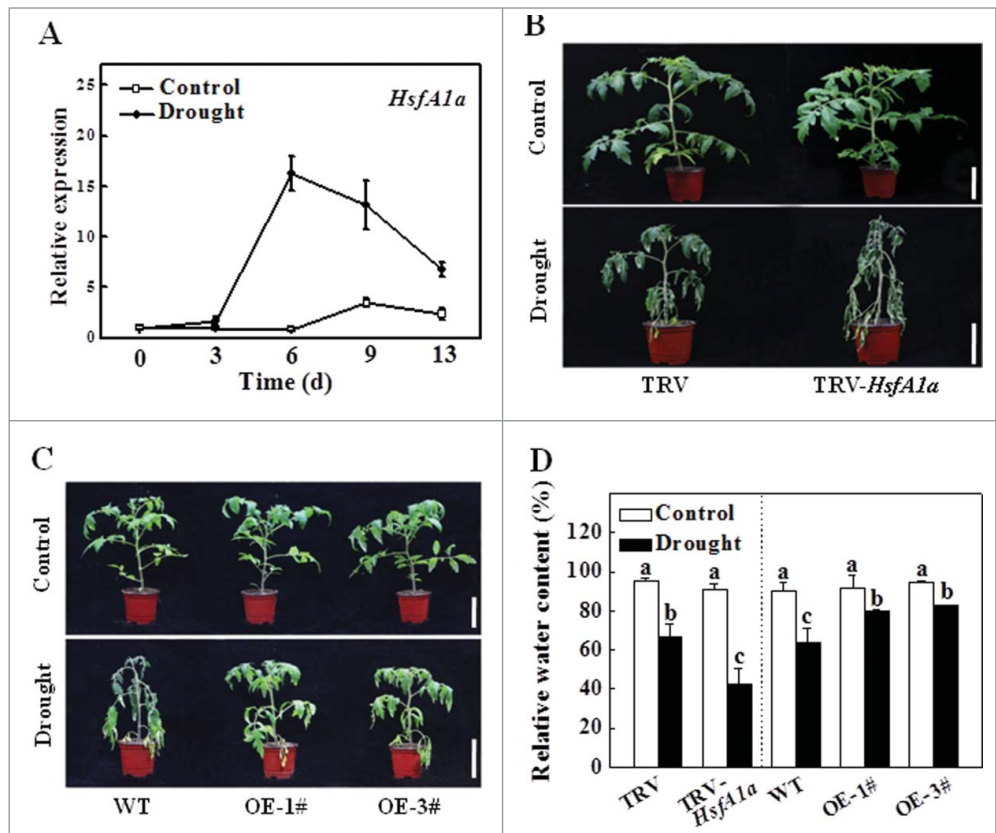


Figure 1. Functional analysis of *HsfA1a* in response to drought stress in tomato leaves. (A) The expression of *HsfA1a* in the WT plants under drought stress. Six-wk-old tomato WT Ailsa Craig plants were exposed to dehydration by withholding water. Total RNA was isolated from leaf samples of the WT plants at the indicated times. (B and C) Reduced or increased tomato drought tolerance in TRV-*HsfA1a* or *HsfA1a*OE plants. Six-wk-old plants in soils were exposed to dehydration by withholding water for 13 d. Bars: 10 cm. (D) Relative water content (RWC) of the terminal leaflets were determined immediately after 13 d of control or drought treatment in TRV and TRV-*HsfA1a* plants or WT and *HsfA1a*OE plants. All data are presented as the means of 5 biological replicates (\pm SE). Means with the same letter did not significantly differ at $P < 0.05$ according to Duncan multiple range test. Three independent experiments were performed with similar results. 1# and 3#, 2 lines of *HsfA1a*OE plants; OE, overexpressing; WT, wild-type.

HsfA1a-silenced plants after 6 d under drought stress (Fig. 2A). Moreover, the ratio of stomatal aperture length over width and ABA accumulation were more increased in TRV-*HsfA1a* plants than that of TRV plants after 6 d under drought stress (Fig. 2B and C). Meanwhile, the stomatal aperture in *HsfA1a*OE plants was higher and ABA contents were significantly decreased when compared with those of WT plants after 6 d under drought stress (Fig. 2D, E and F). These results indicate that endogenous ABA and stomatal closure are more sensitive in TRV-*HsfA1a* plants under drought stress and are therefore not likely to account for *HsfA1a*-mediated tomato drought tolerance.

We have previously reported that compromised stress tolerance of mutants for autophagy and WRKY33 is associated with increased accumulation of ubiquitinated protein aggregates under abiotic stress.^{14,31} Due to the important role of *HsfA1a* in plant tolerance to abiotic stresses, we examined whether there was an increased accumulation of ubiquitinated drought-induced protein aggregates in *HsfA1a*-silenced plants. As shown in Fig. 3A, the levels of insoluble protein aggregates were similar in TRV

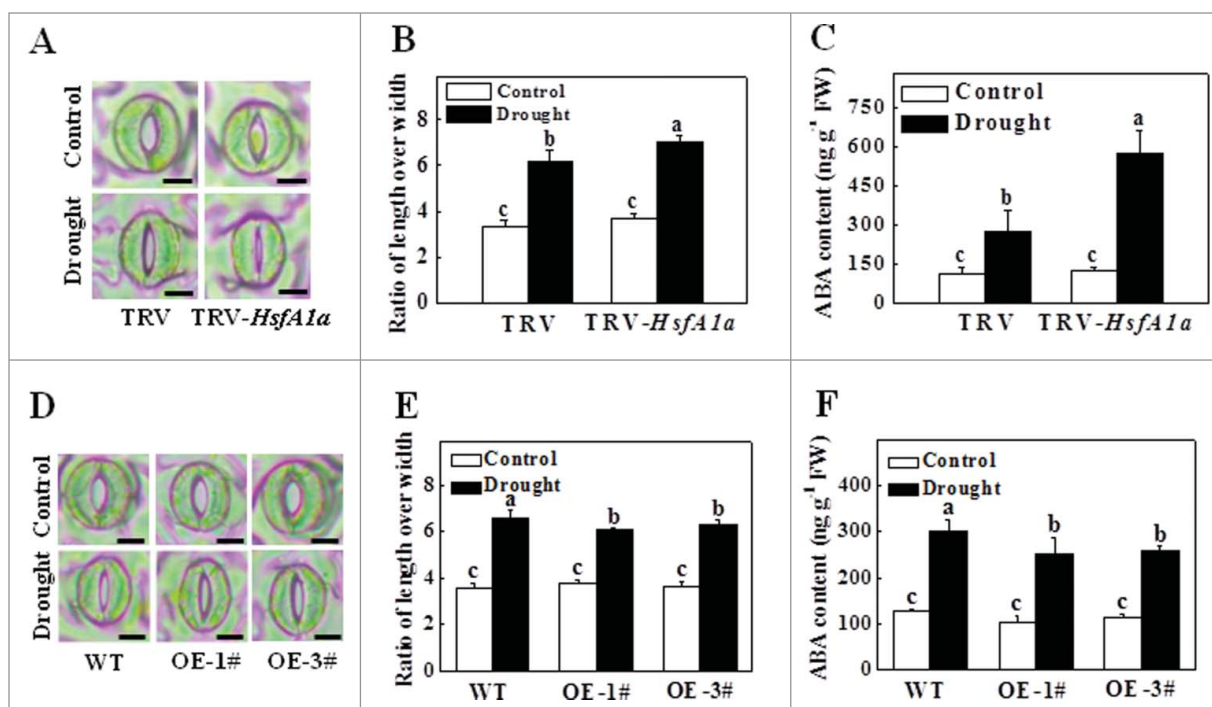


Figure 2. Stomatal aperture and ABA content in TRV-*HsfA1a* and *HsfA1a*OE plants after 6 d under drought stress. (A) Microphotographs of stomata observed in TRV and TRV-*HsfA1a* plants under drought stress. Bars: 10 μ m. (B) Ratio of stomatal aperture length over width were plotted for the TRV and TRV-*HsfA1a* plants under drought stress. The data are presented as the means of 5 biological replicates (\pm SE); each replicate represents the average stomatal aperture of 150 randomly selected stomata. (C) Accumulation of ABA in TRV and TRV-*HsfA1a* plants under drought stress. (D) Microphotographs of stomata observed in WT and *HsfA1a*OE plants under drought stress. Bars: 10 μ m. (E) Ratio of stomatal aperture length over width were plotted for the WT and *HsfA1a*OE plants under drought stress. The data are presented as the means of 5 biological replicates (\pm SE); each replicate represents the average stomatal aperture of 150 randomly selected stomata. (F) Accumulation of ABA in WT and *HsfA1a*OE plants under drought stress. The data are presented as the means of 5 biological replicates (\pm SE). Means with the same letter did not significantly differ at $P < 0.05$ according to the Duncan multiple range test. Three independent experiments were performed with similar results. OE, overexpressing; WT, wild-type.

and TRV-*HsfA1a* plants under normal water supply conditions. However, the level of insoluble protein aggregates in TRV-*HsfA1a* plants was approximately 93.8% higher than in TRV plants after 13 d under drought stress (Fig. 3A). We separated the total proteins to soluble and insoluble proteins and stained with Coomassie brilliant blue. As shown in Fig. S4A, the accumulation of insoluble proteins was increased under drought stress, especially in *HsfA1a*-silenced plants, while, the soluble proteins were decreased which were associated with the increasing of insoluble proteins based on the migration patterns. Thus, the profuse accumulation of insoluble proteins under drought stress was likely to be transferred from the soluble proteins. To determine whether these insoluble proteins were ubiquitinated, we isolated total, soluble and insoluble proteins from TRV and TRV-*HsfA1a* plants collected under normal water supply conditions and after 13 d of drought stress. The proteins were separated with SDS-PAGE and analyzed for ubiquitination using an anti-ubiquitin monoclonal antibody. As shown in Fig. 3B, similar levels of ubiquitinated proteins were observed in the soluble fractions in these plants with or without drought stress. Drought stress induced slight accumulation of ubiquitinated proteins in the insoluble proteins of TRV plants. However, the accumulation of ubiquitinated proteins was drastically increased in the insoluble protein aggregates of TRV-*HsfA1a* plants compared

with the TRV plants after 13 d of drought stress (Fig. 3B). Furthermore, the levels of insoluble protein aggregates did not display significant difference between WT and *HsfA1a*OE plants under normal water supply conditions (Fig. 3C). The levels of insoluble protein aggregates in *HsfA1a*OE-1# and *HsfA1a*OE-3# were 23.1% and 25.4% lower than those of WT plants after 13 d under drought stress (Fig. 3C, Fig. S4B). We also observed similar levels of ubiquitinated proteins in the soluble fractions in WT and *HsfA1a*OE plants with or without drought stress (Fig. 3D). The accumulation of ubiquitinated proteins in the insoluble proteins of *HsfA1a*OE plants were decreased after 13 d withholding water compared with the WT plants (Fig. 3D).

Expression of autophagy-related (*ATG*) genes and formation of autophagosomes under drought stress

To analyze whether autophagy involved in *HsfA1a*-induced drought tolerance, we first examined the expression of 26 autophagy genes identified from the Sol Genomics Network (<http://solgenomics.net/>) in response to drought stress. As shown in Fig. S5, the transcript levels of several *ATG* genes were slightly increased at the 3rd day and most *ATG* gene expression was highly elevated at the 6th day under drought stress when the plants started to show symptoms of dehydration. We compared 20 drought-induced *ATG* genes to further assess the expression

patterns of those genes in *HsfA1a*-silenced and *HsfA1a*OE plants after 6 d under drought stress. As shown in Fig. 4, the transcript levels of these *ATG* genes in TRV-*HsfA1a* or *HsfA1a*OE plants were similar with the levels in TRV or WT plants when they were grown with a normal water supply. However, the expression levels of *ATG10* and *ATG18f* in TRV-*HsfA1a* plants were 50.6% and 64.0% lower than those of TRV plants, respectively, under drought stress conditions (Fig. 4). Furthermore, the expression of *ATG10* and *ATG18f* in *HsfA1a*OE-1# and *HsfA1a*OE-3# plant was significantly increased compared with WT plants after 6 d of drought stress (Fig. 4). Whereas, other 18 *ATG* genes, which were induced by drought stress in WT plants, were similar in VIGS and OE plants when compared with their own control plants (Fig. 4). These results indicated that the expression of many *ATG* genes was induced under drought stress and *ATG10* and *ATG18f* induction under drought stress was *HsfA1a*-dependent.

To investigate the effect of *HsfA1a* on drought-induced autophagy, we used monodansylcadaverine (MDC) as a probe to detect autophagic activity in *HsfA1a*-silenced and -overexpressing plants. MDC is an autofluorescent dye that stains plant autophagosomes.^{14,32} Under normal water supply conditions, we observed low numbers of punctate fluorescent signals in TRV, TRV-*HsfA1a*, WT and *HsfA1a*OE plants (Fig. 5A and B). After a 6-day drought treatment, the numbers of punctate fluorescent signals increased by approximately 2.0- to 2.5-fold in the TRV and WT plants (Fig. 5A and B). Importantly, the number of punctate fluorescence signals after drought stress was substantially reduced in the TRV-*HsfA1a* plants compared to the drought-treated TRV plants (Fig. 5A and C). However, the number of punctate fluorescence signals was significantly increased in *HsfA1a*OE plants compared with the drought-treated WT plants (Fig. 5B and C).

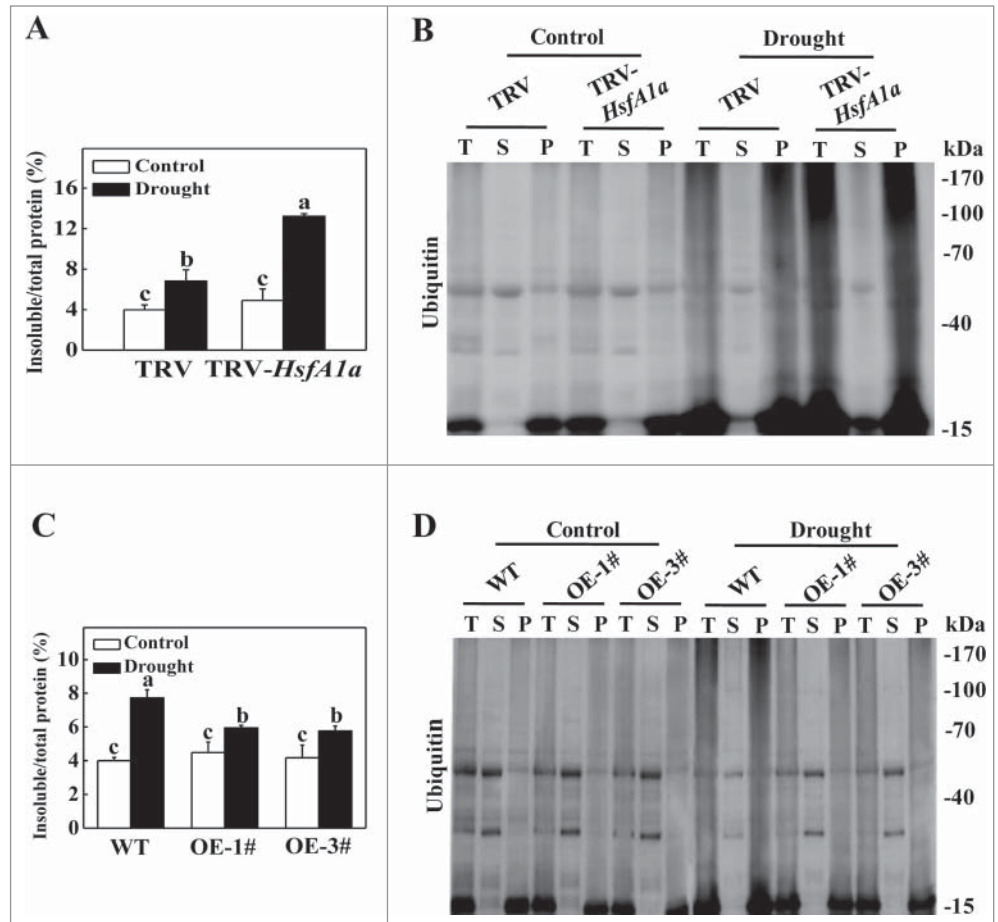


Figure 3. Accumulation and ubiquitination of insoluble proteins in TRV, TRV-*HsfA1a*, WT and *HsfA1a*OE plants under drought stress. (A) Accumulation of insoluble proteins in TRV and TRV-*HsfA1a* plants under drought stress. Leaf tissues from TRV and TRV-*HsfA1a* plants collected at d 13 under drought stress for the preparation of total, soluble and insoluble proteins as described in the Materials and Methods. Total proteins in the starting homogenates and insoluble proteins in the last pellets were determined for the calculation of the percentages of insoluble proteins to total proteins. The data are presented as the means of 5 biological replicates (\pm SE). Means with the same letter did not significantly differ at $P < 0.05$ according to the Duncan multiple range test. (B) Ubiquitination of insoluble protein aggregates in TRV and TRV-*HsfA1a* plants collected at day 13 under drought stress. Proteins from the starting homogenates (T), first supernatant fractions (S) and last pellet fractions (P) were subjected to SDS-PAGE and probed with an anti-ubiquitin monoclonal antibody. Three independent experiments were performed with similar results. (C) Accumulation of insoluble proteins in WT and *HsfA1a*OE plants under drought stress. Leaf tissues from WT and *HsfA1a*OE plants collected at d 13 under drought stress for the preparation of total, soluble and insoluble proteins as described in Materials and Methods. Total proteins in the starting homogenates and insoluble proteins in the last pellets were determined for the calculation of the percentages of insoluble proteins to total proteins. The data are presented as the means of 5 biological replicates (\pm SE). Means with the same letter did not significantly differ at $P < 0.05$ according to the Duncan multiple range test. (D) Ubiquitination of insoluble protein aggregates in WT and *HsfA1a*OE plants collected at day 13 under drought stress. Proteins from the starting homogenates (T), first supernatant fractions (S) and last pellet fractions (P) were subjected to SDS-PAGE and probed with an anti-ubiquitin monoclonal antibody. Three independent experiments were performed with similar results.

To confirm these results, we used transmission electron microscopy (TEM) to monitor autophagic activity under drought stress. In agreement with the results of MDC staining, TEM showed few autophagosomes and autophagic bodies in all of the plants under normal water supply conditions, whereas the numbers of both classic double-membrane autophagosomes in the cytoplasm and signal-membrane autophagic bodies in the

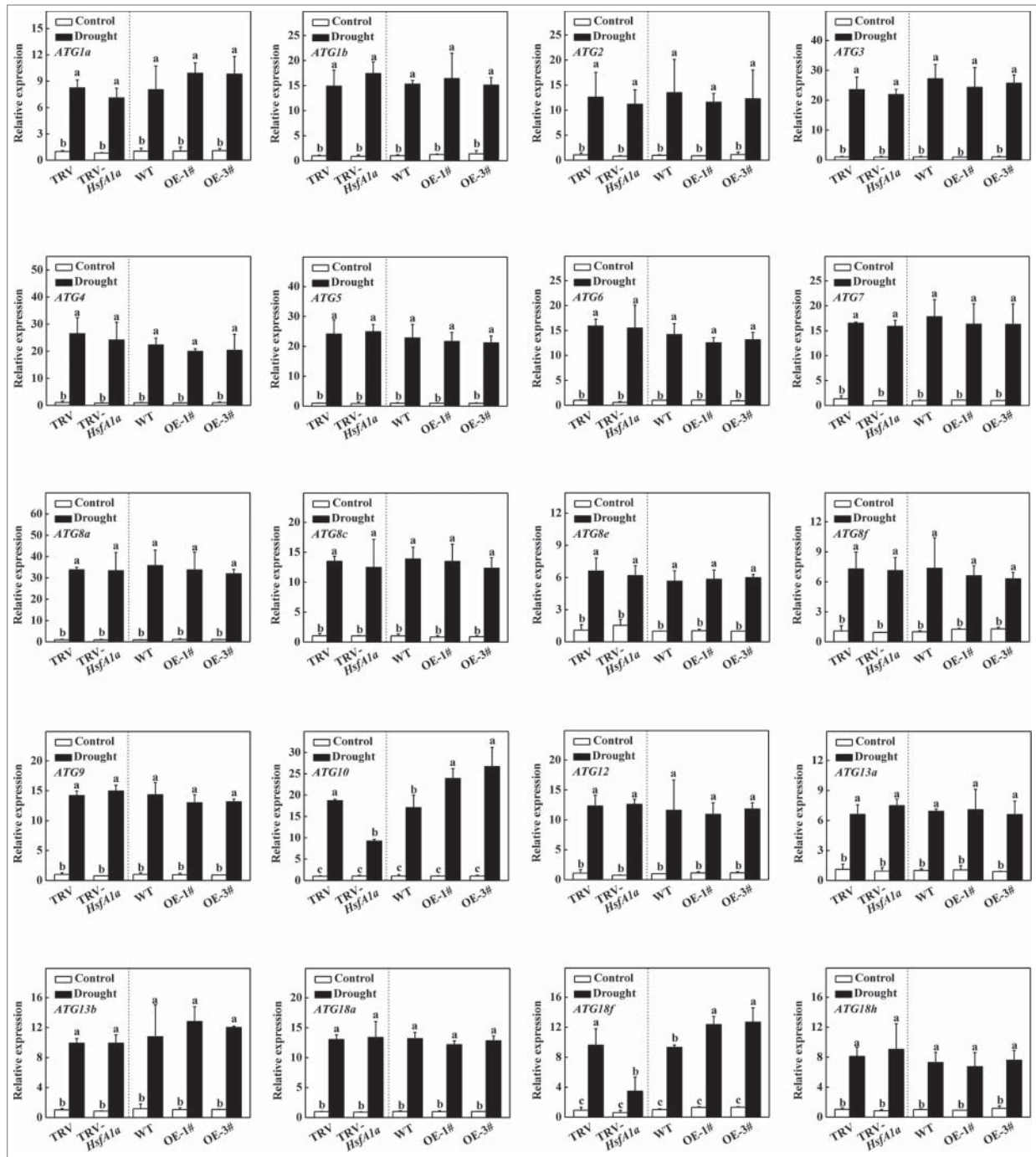


Figure 4. Induction of autophagy genes by drought stress in TRV, TRV-*HsfA1a*, WT and *HsfA1a*OE plants. Six-wk-old tomato plants were exposed to dehydration by withholding water and total RNA was isolated from leaf samples collected on d 6. Transcript levels were determined using qRT-PCR. All data are presented as the means of 5 biological replicates (\pm SE). Means with the same letter did not significantly differ at $P < 0.05$ according to the Duncan multiple range test. Three independent experiments were performed with similar results.

vacuole were increased by 4.0- to 4.5 fold in the TRV and WT plants after 6 d of drought stress (Fig. 5D and E). The number of autophagosomes and autophagic bodies only increased by 1.5-fold in TRV-*HsfA1a* plants, but increased by 9.0-fold in *HsfA1a*OE plants after 6 d of drought stress (Fig. 5D, E and F).

Atg8 has been widely used to monitor autophagosomes. To further examine the induction of autophagy, we used western blotting to analyze the formation of Atg8-phosphatidylethanolamine (PE) conjugates as a marker for autophagic activation using an anti-Atg8a antibody.³³ Under normal water supply conditions, we could barely detect the Atg8-PE band in tomato

plants (Fig. 5G and H). Faster migration of the Atg8-PE bands was observed in TRV and WT plants after 6 d of drought stress (Fig. 5G and H). In contrast, Atg8-PE was significantly decreased in TRV-*HsfA1a* plants but was more abundant in *HsfA1a*OE plants after drought stress (Fig. 5G and H). Taken together, these results suggest that *HsfA1a* is involved in both drought-induced expression of *ATG10* and *ATG18f* genes and autophagosome formation.

Binding of *HsfA1a* to the *ATG10* and *ATG18f* promoters

To examine the possible regulation of tomato *ATG* genes by *HsfA1a*, we inspected 1.5 kb sequences located upstream of the predicted transcriptional start sites of 26 tomato *ATG* genes. Promoters of 5 *ATG* genes (*ATG5*, *ATG8e*, *ATG10*, *ATG13b* and *ATG18f*) contain HSE sequence (GAANN TTC) (Fig. S6). We performed an EMSA to analyze whether *HsfA1a* directly bound in vitro to these promoters. The signaling of probe-protein complex was not detected using *ATG5*, *ATG8e* and *ATG13b* probes (data not shown). However, *HsfA1a* bound to the *ATG10* and *ATG18f* promoter probes (Fig. 6). When the core sequence of HSE motif²⁶ in the *ATG10* probe was mutated to the mutant *ATG10*-1 Δ probe (Fig. 6A), the binding to the complex was reduced (Fig. 6B). When additional mutations were introduced to the mutant *ATG10*-2 Δ probe (Fig. 6A), the binding by *HsfA1a* was totally lost (Fig. 6B). Similarly, the binding signal to the complex was not detected when the HSE sequence in the *ATG18* probe was mutated to the mutant *ATG18f* Δ probe (Fig. 6A and C). These results suggest that the *HsfA1a* protein specifically binds to the HSE sequences in the synthesized probes of the *ATG10* and *ATG18f* promoters *in vitro*.

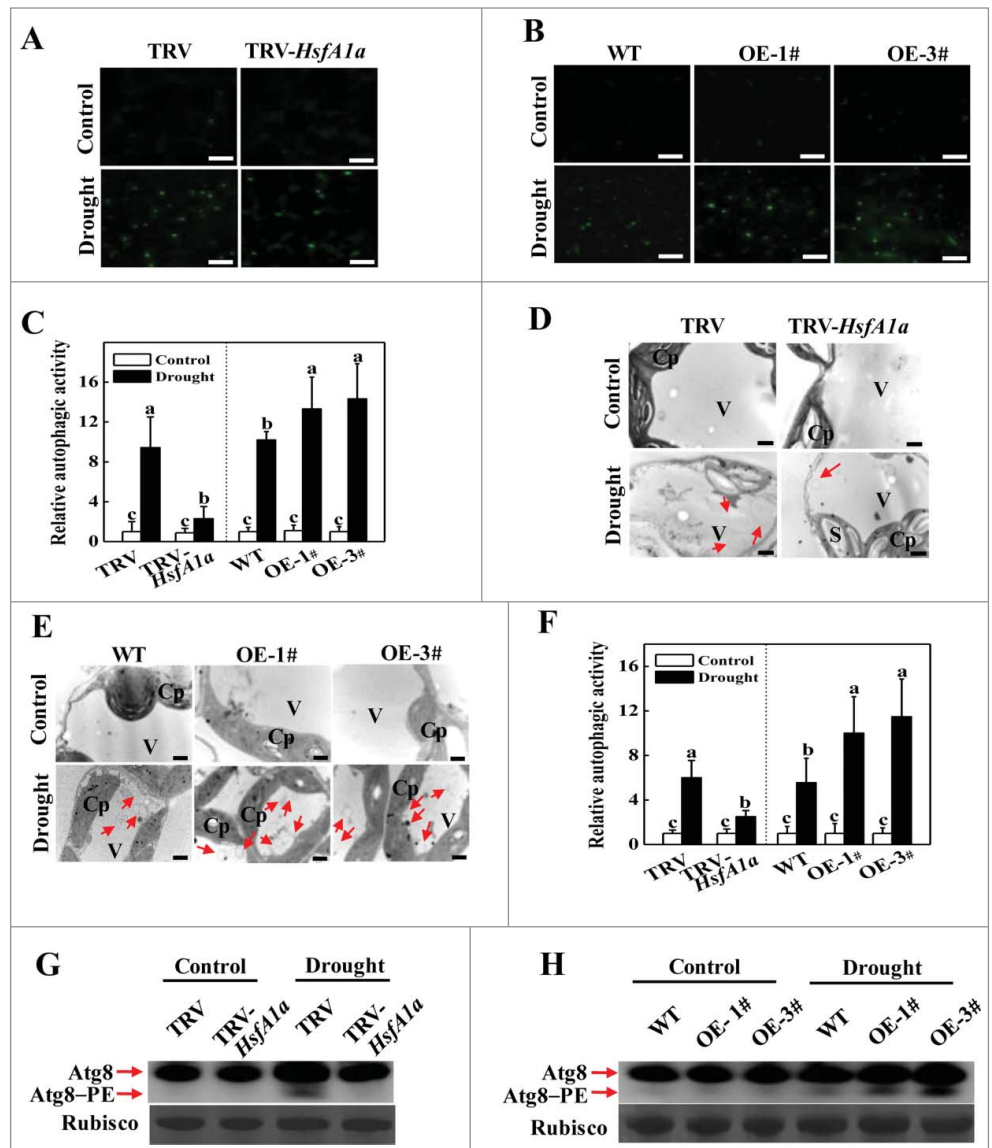


Figure 5. Visualization of the accumulation of autophagosomes in tomato leaves under drought stress. **(A and B)** MDC-stained autophagosomes in the leaves of TRV and TRV-*HsfA1a* or WT and *HsfA1a*OE plants. Six-wk-old plants were exposed to dehydration by withholding water and the leaves were MDC-stained and visualized on day 6 by fluorescence confocal microscopy. MDC-labeled structures are shown as green signals. Bars: 25 μ m. **(C)** Relative autophagic activity normalized to the activity of the TRV or WT control plants in **(A and B)**. The MDC-stained autophagosomes in leaves at each treatment were quantified to calculate the autophagic activity relative to TRV or WT control plants, which was set to 1. More than 300 mesophyll cells for each treatment were used for the quantification. **(D and E)** Representative transmission electron microscopy (TEM) images of autophagic structures in the mesophyll cells of TRV and TRV-*HsfA1a* or WT and *HsfA1a*OE plants. Six-wk-old plants were exposed to dehydration by withholding water and the mesophyll cells were visualized on d 6 by TEM. Autophagic bodies are indicated by red arrows. Bars: 1 μ m. **(F)** Relative autophagic activity normalized to the activity of the TRV or WT control plants in **(D and E)**. More than 20 cells were used to quantify autophagic structures. **(G and H)** Atg8 protein levels in the leaves of TRV and TRV-*HsfA1a* plants or WT and *HsfA1a*OE plants. Atg8 and Atg8-PE are the nonlipidated and lipidated forms of Atg8, respectively. The Rubisco large subunit was used as a loading control for the western blotting analysis. Results represent the means \pm SE. Means with the same letter did not significantly differ at $P < 0.05$ according to the Duncan multiple range test. Three independent experiments were performed with similar results. Cp, chloroplast; V, vacuole; S, starch; OE, overexpressing; WT, wild-type; 1# and 3#, 2 lines of *HsfA1a*OE plants.

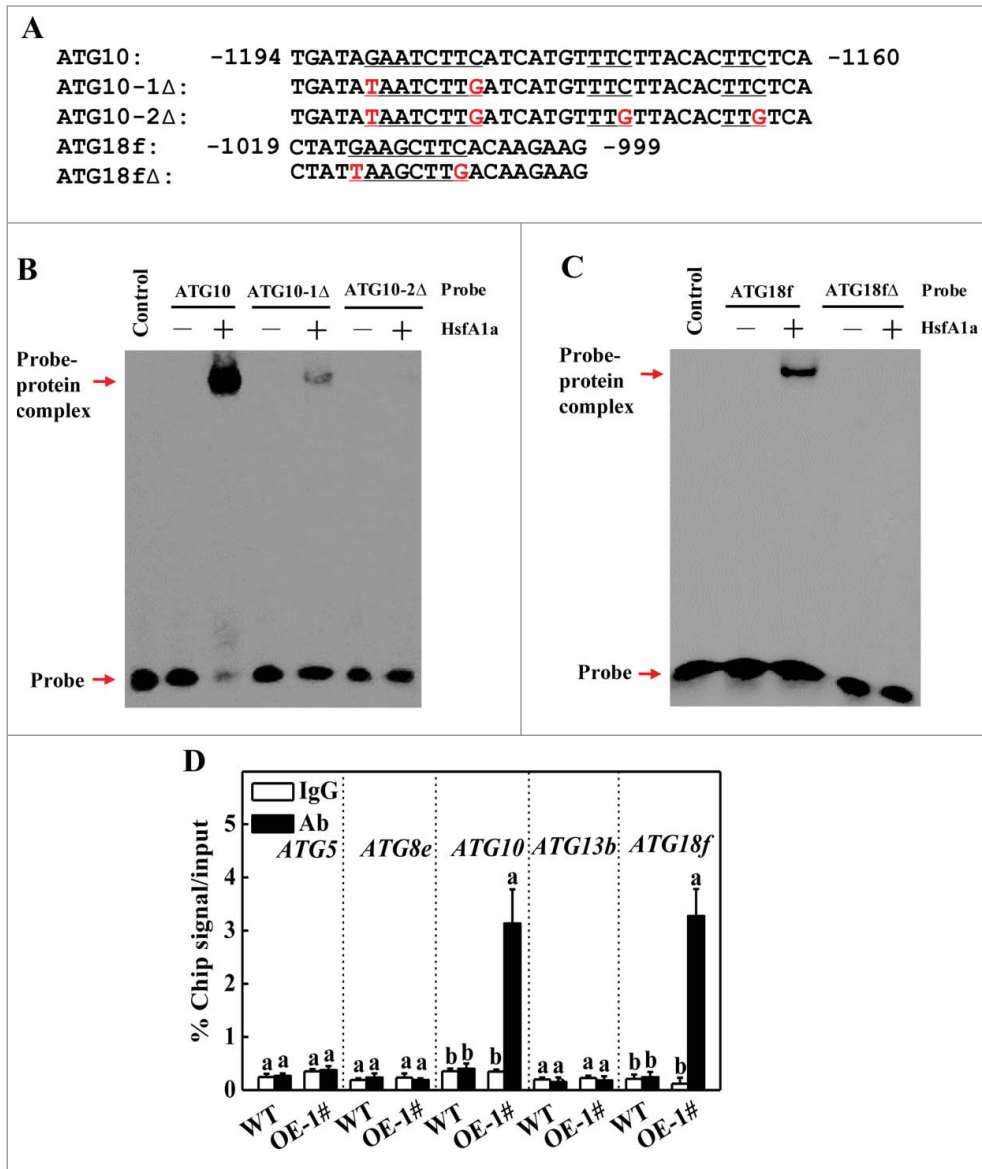


Figure 6. HsfA1a binds to the promoters of *ATG10* and *ATG18f* *in vitro* and *in vivo*. (A) Oligonucleotide used in the electrophoretic mobility shift assays (EMSA). The ATG10 probe contains one direct HSE, whereas in the ATG10-1Δ and ATG10-2Δ probes the HSE core sequence was mutated. The ATG18f probe contains one direct HSE, whereas in the ATG18fΔ probe, the HSE core sequence was mutated. The WT and mutated HSE sequences are underlined. The mutated bases were indicated in red. (B and C) EMSA showing HsfA1a bound to the HSE sequences of the *ATG10* or *ATG18f* promoters. Recombinant HsfA1a was purified from *E. coli* cells and used for DNA binding assays with ATG10, ATG10-1Δ, ATG10-2Δ, ATG18f, or ATG18fΔ as the probes. His was included as the negative control. (D) Direct binding of HsfA1a to the *ATG10* and *ATG18f* promoters was analyzed using ChIP-qPCR in *35S-HsfA1a-HA*-overexpressing (*HsfA1a*OE) plants. Six-wk-old *HsfA1a*OE plants were exposed to dehydration by withholding water and input chromatin was isolated from leaf samples on d 6. The epitope-tagged HsfA1a-chromatin complex was immunoprecipitated with an anti-HA antibody. A control reaction was processed side-by-side using mouse IgG. Input- and ChIP-DNA samples were quantified by qRT-PCR using primers specific for the promoters of the *ATG* genes. The ChIP results are presented as percentage of the input DNA. Means with the same letter did not significantly differ at $P < 0.05$ according to the Duncan multiple range test. Three independent experiments were performed with similar results. OE, overexpressing; 1#, line of *HsfA1a*OE plants.

To determine whether tomato HsfA1a directly regulates the expression of these 5 *ATG* genes *in vivo*, we performed ChIP-qPCR assays to test HsfA1a protein binding to the promoters of

these *ATG* genes under drought stress. As shown in Fig. 6D, only *ATG10* and *ATG18f* promoter sequences were substantially enriched using an anti-HA antibody that immunoprecipitated the 3HA-tagged HsfA1a transgene product in the OE lines and not the WT lines after 6 d of drought stress. In contrast, the IgG control antibody failed to pull down these 2 *ATG* gene promoter DNA segments (Fig. 6D). Thus, HsfA1a binds to the *ATG10* and *ATG18f* gene promoters and may directly regulate their induction under drought stress.

Identification and functional analysis of *ATG10* and *ATG18f* in HsfA1a-induced tolerance and formation of autophagosomes under drought stress

To test the functions of the *ATG10* and *ATG18f* genes in HsfA1a-induced drought tolerance, *ATG10* and *ATG18f* genes were respectively silenced in WT and *HsfA1a*OE plants, and the expression of their own gene was decreased 60 to 70% in silenced plants compared with their own TRV control plants (Fig. S7A). Silencing of *ATG10* or *ATG18f* gene did not affect *HsfA1a* gene expression under normal water supply condition or drought stress (Fig. S7B). No significant differences in phenotypes, RWC and EL were observed in the *ATG10*- and *ATG18f*-silenced plants compared with TRV control plants under normal water supply condition (Fig. S7C to E). However, most of the leaves from *ATG10*- and *ATG18f*-silenced WT and *HsfA1a*OE plants exhibited serious wilting after 13 d of drought stress (Fig. S7C). The RWC of the TRV-*ATG10* and pTRV-*ATG18f* plants were 30.9% and 15.4%

lower than WT TRV plants after 13 d of drought stress, respectively (Fig. S7D). Similarly, the RWC of the *HsfA1a*OE TRV-*ATG10* and TRV-*ATG18f* plants were decreased by 30.9% and

31.6% compared with the *HsfA1a*OE TRV plants, respectively (Fig. S7D). Similarly, the EL values of the TRV-*ATG10* and TRV-*ATG18f* plants were increased by 35.4% and 12.1%, respectively, compared with the WT TRV plants (Fig. S7E). The EL values of the *HsfA1a*OE TRV-*ATG10* and TRV-*ATG18f* plants were 131.2% and 147.2% higher than those of *HsfA1a*OE TRV plants (Fig. S7E).

To further investigate the role of the *ATG10* and *ATG18f* genes in the *HsfA1a*-mediated drought stress response, we used MDC and TEM to detect autophagic activity. We observed low numbers of punctate fluorescent signals in all of the plants under normal water supply conditions (Fig. 7A). The numbers of punctate fluorescent signals significantly increased in WT TRV plants after a 6-d drought treatment (Fig. 7A and B). However, the number of punctate fluorescence signals in all TRV-*ATG10* and TRV-*ATG18f* plants was decreased by 66.7 to 73.4%. Furthermore, the TEM results were in agreement with the results MDC staining results. Under normal water supply conditions, few autophagosomes and autophagic bodies were detected in any of the plants. The numbers of autophagosomes and autophagic bodies increased by 6-fold in WT TRV plants. However, the numbers of autophagosomes and autophagic bodies in TRV-*ATG10* and TRV-*ATG18f* plants increased only by 2.1- to 2.5-fold under drought stress (Fig. 7C and D). Thus, *HsfA1a*-induced drought tolerance and formation of autophagosomes under drought stress were largely *Atg10*- and *Atg18f*-dependent.

Discussion

Studies over the past 20 years have provided a large body of evidence that autophagy plays a critical role in a wide range of important biological processes in plants.^{9,13} In

contrast, our understanding of the regulation of autophagy in plants is extremely limited. In the present study, we provided genetic evidence that *HsfA1a*, a transcription factor involved in plant stress responses, contributed to the upregulation of autophagy genes and the formation of autophagosomes. Furthermore, autophagy was involved in *HsfA1a*-mediated tomato drought tolerance. These results provide important new insights into the regulation of autophagy in plant stress responses.

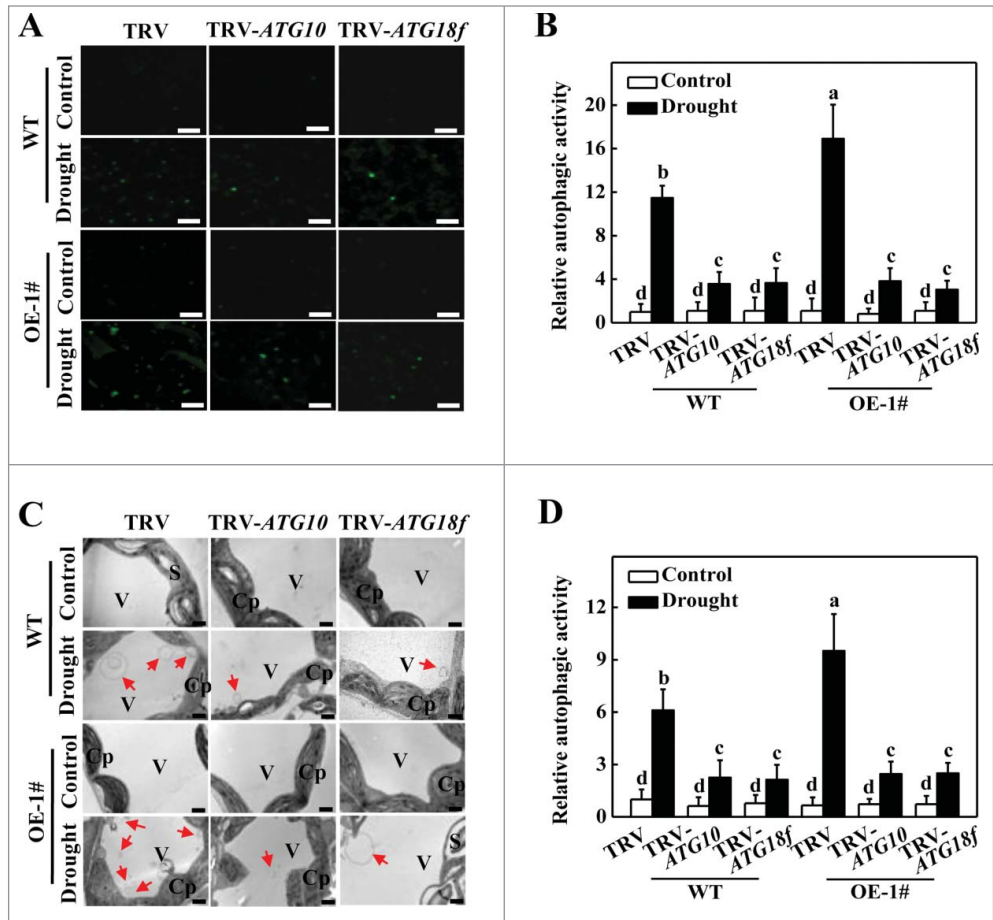


Figure 7. Visualization of the accumulation of autophagosomes by confocal microscopy and transmission electron microscopy (TEM) in *ATG10* and *ATG18f*-silenced plants under drought stress. (A) MDC-stained autophagosomes in the leaves of WT TRV, TRV-*ATG10* and TRV-*ATG18f* plants or *HsfA1a*OE TRV, TRV-*ATG10* and TRV-*ATG18f* plants. Six-wk-old plants were exposed to dehydration by withholding water and the leaves were MDC-stained and visualized on day 6 by fluorescence confocal microscopy. MDC-labeled structures are visible as green signals. Bars: 25 μ m. (B) Relative autophagic activity normalized to the activity of WT TRV control plants in (A). Quantification of the MDC-stained autophagosomes in the leaves at each treatment was performed to calculate the autophagic activity relative to WT TRV control plants, which was set to 1. More than 300 mesophyll cells for each treatment were used for the quantification. (C) TEM images of autophagic structures in the mesophyll cells of WT TRV, TRV-*ATG10* and TRV-*ATG18f* plants or *HsfA1a*OE TRV, TRV-*ATG10* and TRV-*ATG18f* plants. Six-wk-old plants were exposed to dehydration by withholding water and the mesophyll cells were visualized on d 6 by TEM. Autophagic bodies are indicated by red arrows. Bars: 1 μ m. (D) Relative autophagic activity normalized to the activity in WT TRV control plants in (C). More than 20 cells were used to quantify autophagic structures. Results represent the means \pm SE. Means with the same letter did not significantly differ at $P < 0.05$ according to the Duncan multiple range test. Three independent experiments were performed with similar results. Cp, chloroplast; V, vacuole; S, starch; WT, wild-type; OE, overexpressing; 1#, line of *HsfA1a*OE plants.

Water scarcity has a dramatic impact on crop growth and productivity.³⁴ The phytohormone ABA is produced under water-deficit conditions and plays an important role in the adaptation of vegetative tissues to drought.³⁵ ABA promotes stomatal closure in guard cells to reduce transpiration and conserve water, and regulates the expression of many genes that may function in plant dehydration tolerance.³⁶ Additionally, various transcription factors play critical roles in plant signaling networks to regulate plant drought tolerance and activate gene transcription and the downstream metabolic system.³⁷ The present study demonstrated that drought stress induced the expression of transcription factor *HsfA1a* and silencing of the *HsfA1a* gene made tomato plants hypersensitive to drought stress, while overexpression of the *HsfA1a* gene increased plant drought tolerance (Fig. 1). Collectively, these results indicate that transcription factor HsfA1a plays a critical role in plant drought tolerance. Silencing of the *HsfA1a* gene resulted in an increased reduction of the stomatal aperture compared to the TRV control under drought stress, whereas drought stress induced increased levels of ABA accumulation in TRV-*HsfA1a* plants compared to the TRV control plants (Fig. 2). These results argued against a critical role of ABA-dependent pathways in HsfA1a-mediated plant drought tolerance.

Drought stress is an important threat to plant protein activities through diminution in cellular volume, macromolecular crowding and oxidative damage.³⁸ Abiotic stresses, such as drought, cause damage to a variety of cellular structures and macromolecules, including protein denaturation and aggregation.³⁹ Molecular chaperones, such as Hsp70, and the LEA proteins (which bind with high affinity to solvent-exposed, nonstructural and hydrophobic regions of denatured proteins), can maintain targeted proteins in their functional conformations and prevent the aggregation of denatured proteins, thereby contributing to cellular homeostasis under mild to moderate stress conditions.^{40,41} Numerous studies have shown that stress-generated misfolded proteins that cannot reestablish their normal conformation are recognized, ubiquitinated and targeted for degradation by the cellular protein quality control machinery.^{31,42,43} We have previously observed that denatured or otherwise damaged cellular proteins are ubiquitinated under heat and oxidative stress conditions in *Arabidopsis* plants.⁴³ Ubiquitination is an enzymatic protein post-translational modification (PTM) process in which ubiquitin (Ub, a highly conserved 8-k_D protein) is attached to substrate proteins, such as denatured or damaged cellular proteins, in 3 consecutive steps catalyzed by the E1, E2, and E3 enzymes.^{44,45} Here, we observed a significant increase in the level of insoluble proteins in TRV-*HsfA1a* plants compared with the TRV control plants (Fig. 3A). Under drought stress, the TRV-*HsfA1a* plants but not the TRV control plants displayed a major elevation in the levels of ubiquitinated proteins (Fig. 3B), indicating that drought-induced ubiquitinated proteins are aggregated and accumulated in *HsfA1a*-silenced plants due to reduced degradation.

For targeted degradation, aggregated or damaged proteins formed under stress conditions must be specifically recognized and transferred to the protein degradation systems. When native

structures cannot be achieved, molecular chaperones can facilitate their degradation through association with chaperone-dependent ubiquitin E3 ligases that can specifically catalyze the ubiquitination of denatured or misfolded but not native proteins in a chaperone-dependent manner.⁴⁶ Ubiquitinated proteins can be degraded by the UPS and autophagic pathway.^{31,47, 48} However, the UPS is limited in its capacity to degrade oligomeric and aggregated proteins that are not sufficiently small to fit through the narrow proteasome entrance channel.⁴⁹ The increased accumulation of ubiquitinated proteins in drought- and heat-treated autophagy mutants indicates that autophagy is also a major mechanism underlying the degradation of ubiquitinated proteins under stress conditions in plants.³¹ Indeed, drought stress induced an increase in the transcript levels of *ATG* genes (Fig. S5) and the formation of autophagosomes in WT tomato plants (Fig. 5B and E). Moreover, the accumulation of ubiquitinated aggregates in *HsfA1a*-silenced plants was associated with compromised autophagosome formation (Figs. 3B and 5A and D). The expression of most *ATGs* was still induced under drought stress; however, induction of *ATG10* and *ATG18f* gene expression was compromised in TRV-*HsfA1a* plants under drought stress (Fig. 4), indicating that HsfA1a is necessary for the sustained induction of autophagy in the plant response to drought stress.

The oligomerization domain of HsfA1a is required for the formation of functional trimers under stress conditions,⁵⁰ which can then bind to the HSEs of target genes and regulate their transcription.⁵¹ The expression of *ATG10* and *ATG18f* was compromised in TRV-*HsfA1a* plants under drought stress, and, interestingly, the promoters of these genes contained HSE boxes (Fig. 6A). HsfA1a directly bound the HSE boxes in the promoters of these 2 autophagy genes based on results from *in vitro* EMSA and *in vivo* ChIP-qPCR assays (Fig. 6B to D), indicating that *ATG10* and *ATG18f* are direct target genes of the HsfA1a transcription factor. In *Arabidopsis*, Atg10 has been identified as the Atg12-conjugating enzyme that was essential for autophagic vesicle formation.⁵² *atg10* mutant plants are hypersensitive to nitrogen and carbon starvation and fail to accumulate autophagic bodies inside the vacuole.⁵² In the present study, genomic database searches with BLASTP identified a single tomato *ATG10* gene that contained several regions with strong amino acid conservation, including a presumed active-site cysteine (Cys176) that forms the thioester intermediate with Atg12 prior to its transfer to Atg5.⁵² Silencing of the tomato *ATG10* gene made the plants hypersensitive to drought stress (Fig. S7) and blocked autophagy formation under drought stress (Fig. 7). The plant *ATG18f* gene is a member of the *ATG18* gene family and possesses a sequence similar to the yeast autophagy gene *ATG18*.⁵³ In *Arabidopsis*, the transcript level of *ATG18f* was upregulated during nutrient starvation and a combination of drought and heat stress,^{53,54} indicating that Atg18f potentially played a role in the response to these stress conditions. Indeed, silencing of the tomato *ATG18f* gene compromised plant tolerance against drought stress (Fig. S7) and inhibited autophagosome formation (Fig. 7). Thus, the Atg18f protein is likely to be required for autophagosome formation in

tomato plants. Importantly, *ATG10*- or *ATG18f* silencing in *HsfA1a*-overexpressing plants resulted in hypersensitivity to drought stress and completely blocked *HsfA1a*-mediated plant drought tolerance (Fig. S7). Likewise, induced autophagy formation in *HsfA1a*-overexpressing plants was significantly reduced by silencing *ATG10* or *ATG18f* (Fig. 7), supporting that the *ATG10* and *ATG18f* were involved in *HsfA1a*-mediated formation of autophagosomes and drought tolerance. In human breast adenocarcinoma cells, HSF1 (heat-shock factor 1), a master regulator of the heat-shock responses in mammal, was identified as the regulator of cytoprotective autophagy induced by the chemotherapeutic agent carboplatin through an increase in LC3 punctate structures and LC3 and Atg7 protein expression.⁵⁵ Thus, the transcriptional upregulation of autophagy genes does not appear to be as independent in plants as the process observed in mammalian systems.

During the plant stress response, *HsfA1a* interacts with *HsfA2* to form hetero-oligomeric complexes that can synergistically regulate the expression of some *Hsfs* and molecular chaperone *Hsps*, including a number of small *Hsps*, *DnaJ/Hsp40*, and *Hsp70*.^{22,25,56,57} These chaperones assist with a wide range of protein-folding processes to prevent protein aggregation in plant cells under normal and stress conditions.⁴¹ The transcript levels of several Hsp-encoding genes are significantly reduced in *Arabidopsis hsfA1a* and *hsfA1b* double-knockout mutants,⁵¹ indicating that *HsfA1s* play a positive role in protein folding and in preventing aggregation through the regulation of molecular chaperone *Hsps*. Indeed, silencing of *HsfA1a* induced the accumulation of insoluble protein aggregates in tomato plants under drought stress, and these proteins were highly ubiquitinated (Fig. 3). We have previously observed that silencing of the tomato autophagy genes *ATG5* and *ATG7* or tomato autophagy receptors *NBR1a* and *NBR1b* significantly reduces the heat-induced transcript levels of some Hsp-encoding genes,¹⁴ indicating that the formation of autophagosomes has a positive feedback effect on the upregulation of *Hsfs*-activated *Hsps*. Thus, *HsfA1a* has dual functions in the regulation of protein aggregates and proteotoxicity in the plant stress response, including the stabilization of unfolded proteins, the prevention of unwanted protein aggregation through the transcriptional upregulation of molecular chaperones *Hsps*, and the degradation of stress-induced protein aggregation through induction of some autophagy genes and the formation of autophagosomes.

In conclusion, we have provided comprehensive genetic and molecular analyses of tomato *HsfA1a* in induced autophagy and plant drought tolerance (Fig. 8). We demonstrated that *HsfA1a* acts as a positive regulator of the expression of the autophagy genes *ATG10* and *ATG18f* and the formation of autophagosomes during induction of autophagy under stress conditions, such as drought. Stress-damaged proteins or protein aggregates are recognized and polyubiquitinated by specific E3 ubiquitin ligases and delivered to the expanding phagophores. Expansion and closure of the phagophores result in the formation of autophagosomes, which then can fuse with vacuoles to form autophagic vacuoles in which ubiquitinated proteins or protein aggregates are degraded (Fig. 8). Processing and degradation of stress-induced protein

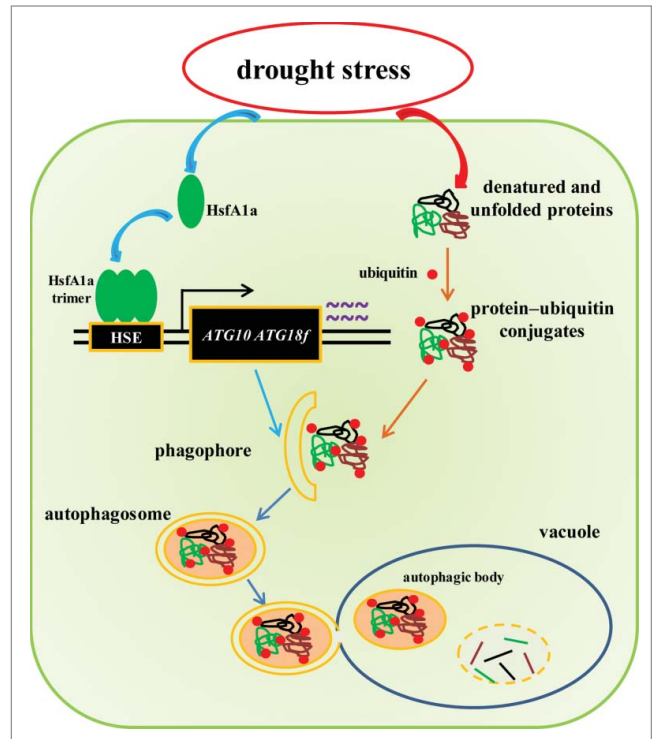


Figure 8. A proposed model for the induction of autophagy by *HsfA1a* in tomato plants under drought stress. *HsfA1a* is first activated under drought stress by increasing transcription and trimer formation. Then, activated *HsfA1a* binds to and upregulates the expression of *ATG10* and *ATG18f* leading to an increase in autophagy. The increase in autophagy leads to an increase in the degradation of insoluble ubiquitinated protein aggregates and cell survival under drought stress.

aggregates would increase stress tolerance, leading to increased survival of plants under stress conditions.

Materials and Methods

Plant materials and experimental design

The tomato *Solanum lycopersicum* cv. Ailsa Craig genotype was used in all experiments. Seeds were germinated and grown in 250 cm³ plastic pots filled with a mixture of peat and vermiculite (2:1, v:v). The plants were watered daily with Hoagland nutrition solution in the chamber. The growth conditions were as follows: a 14/10 light/dark cycle, 23/21°C day/night temperature, and 600 μmol m⁻² s⁻¹ photosynthetic photon flux density (PPFD).

To induce drought stress, plants in soil were watered to saturation and then exposed to dehydration by withholding water for 13 d. During drought periods, the relative soil water content was measured using a ZigWSN recorder (Ziteng, China) daily to ensure that every pot maintained the same level of water content.

Generation and selection of transgenic plants

To obtain the tomato *HsfA1a* overexpression construct, the 1581 bp full-length coding DNA sequence (CDS) was amplified

with the primers *Hsf1a*OE-F (5'-TTGGCGCGCCATGGAGCCGAATTCCTTAT-3') and *Hsf1a*OE-R (5'-GGGGTACCGATCATATGTTTTTGTG-3') using tomato cDNA as the template. The PCR product was digested with *Ascl* and *KpnI* and inserted behind the CaMV 35S promoter in the plant transformation vector pFGC1008-HA. The resulting *Hsf1a*OE-HA plasmid was transformed into *Agrobacterium tumefaciens* strain EHA105. Tomato seeds of Ailsa Craig were used for transformation, as described by Fillatti et al.⁵⁸ Transgenic plants overexpressing the *Hsf1a* transgene were identified by western blotting using an anti-HA (Pierce, 26183) monoclonal antibody (Fig. S1). Two independent homozygous lines of the F2 progeny were used in the study.

VIGS constructs and *Agrobacterium*-mediated virus infection

TRV VIGS constructs were used to silence the tomato *Hsf1a*, *ATG10*, and *ATG18f* genes. These genes were generated by PCR amplification using gene-specific primers (Table S1), digested with the appropriate restriction enzymes and ligated into the same sites in TRV2. The resulting plasmids were transformed into *Agrobacterium tumefaciens* strain GV3101. *A. tumefaciens*-mediated virus infection was performed as previously described.⁵⁹ The plants were kept at 22°C and used for experiments 3 wk after *A. tumefaciens* infiltration. Leaflets in the middle of the fifth fully expanded leaves, which showed about 30 to 40% transcript levels of control plants, were used.

Stomatal conductance and relative water content determination

Stomatal conductance was detected according to Xia et al.⁶⁰ After 6 d drought, tomato leaves abaxial epidermises were peeled with forceps and floated on buffer (30 mM KCl, 10 mM 2-[N-morpholino]-ethanesulfonic acid [MES], pH 6.15). The stomatal apertures were measured using a light microscope equipped with a digital camera (Leica Microsystems, Germany).

The leaves of relative water content was measured according to Zhou et al.⁶¹ The fresh weights of the terminal leaflets were measured as Fw. Then, the leaves were immersed in distilled water in darkness for 24 h to obtain the fully turgid weight (Tw). Leaves were dried in an oven at 70°C for 48 h and weight the dry weight (Dw). The relative water content was calculated as follows: RWC (%) = (Fw-Dw)/(Tw-Dw) × 100.

ABA measurements

ABA contents were measured according to Welsch et al.⁶² with modification. Briefly, 0.3 g of frozen leaf tissues was ground and homogenized in 3 ml of ethyl acetate containing 100 ng ml⁻¹ [²H₆](+)-cis,trans-ABA (OChemlm Ltd., 35671-08-0) as an internal standard. The homogenate was shaken for 12 h in the dark at 4°C and then centrifuged at 15,000 × g for 10 min. The supernatant fraction was transferred to a new tube; then, the pellet was re-extracted with 3 ml of ethyl acetate and combined with the supernatant fraction. The supernatant fraction was eluted through a Sep-Pak C18 cartridge (Waters, WAT020805) to remove the polar compounds and dried under nitrogen. Dried samples were resuspended in 0.5 ml of 70% methanol (v/v). Then, the samples (20 μL) were analyzed by HPLC electrospray ionization/MS-MS using an Agilent 1290 HPLC (Agilent

Technologies, Germany) coupled to an Agilent 6460 triple Quad LC/MS (Agilent Technologies, Germany). Chromatographic separation was performed on an Agilent XDB 3.5 μm C18 150 mm × 2.1 mm column at 40°C. The solvent gradient consisted of solvent A (0.1% formic acid aqueous water) and solvent B (100% methanol) at a flow rate of 0.3 ml/min over 20 min with the following gradient setup: 0 to 1.5 min, A: B at 60: 40; a 6.5 min; switch to A: B of 0: 100; and the return of solvent A: B to 60: 40 for 5 min until the end of the run. [²H₆](+)-cis,trans-ABA was used to estimate the recovery rate of the ABA content, which was quantified using the external standard.

Total RNA extraction and gene expression analysis

Total RNA was isolated from tomato leaves using RNAsimple Total RNA Kit (Tiangen, DP419) according to the manufacturer's instructions. Total RNA (1 μg) was used to reverse transcribed for cDNA template using the ReverTra Ace qPCR RT Kit (Toyobo, FSQ-301).

The qRT-PCR assays were performed using an LightCycler® 480 II Real-Time PCR detection system (Roche, Swiss). PCRs were performed using the SYBR Green PCR Master Mix (Takara, RR420A). The PCR conditions consisted of denaturation at 95°C for 3 min, followed by 40 cycles of denaturation at 95°C for 15 s, annealing at 58°C for 15 s and extension at 72°C for 30 s. The tomato *Ubi3* gene was used as an internal control. Gene-specific primers were designed according to cDNA sequences as described in supplemental Table S2. Relative gene expression was calculated as described as Livak and Schmittgen.⁶³

Protein extraction and western blotting

For protein extraction, tomato leaves were ground in liquid nitrogen and homogenized in extraction buffer (100 mM Tris-HCl, pH 8.0, 10 mM NaCl, 1 mM EDTA, 1% Triton X-100 [Aladdin, T109026], 1 mM phenylmethylsulphonyl fluoride and 0.2% β-mercaptoethanol). The soluble, insoluble and ubiquitinated proteins were detected as described as our previous study.³¹ The homogenates were filtered through a 300-μm and then 100-μm nylon mesh. Half of the filtered samples were kept to detect total proteins. Other samples were clarified by centrifugation at 2,200 × g for 5 min. Supernatant fractions were kept to detect soluble proteins. The pellet fractions were resuspended in the same buffer and subjected to the low speed centrifugation. The process was repeated twice and after the last centrifugation the pellet fractions were resuspended to detect insoluble protein. The concentrations of proteins in the homogenates (total proteins), the first supernatant fractions (soluble proteins) and last pellet fractions (insoluble proteins) were determined using Bio-Rad protein assay kit (500-0001). The denatured protein extracts were separated using 12% sodium dodecyl sulfate-polyacrylamide gel electrophoresis (SDS-PAGE). For Atg8a detection, the denatured protein was separated on a 13.5% SDS-PAGE gel in the presence of 6 M urea. For western blotting, the proteins on the SDS-PAGE gel were transferred to a nitrocellulose membrane. The membrane was blocked for 1 h in TBS buffer (20 mM Tris, pH 7.5, 150 mM NaCl, and 0.1% Tween 20 [Amresco, 0777]) with 5% skim milk powder at room

temperature, and then incubated for 1 h in TBS buffer with 1% BSA (Amresco,0332) containing a mouse anti-ubiquitin monoclonal antibody (Sigma-Aldrich, U0508), or rabbit anti-Atg8a polyclonal antibody (Abcam, ab77003). After incubation with a goat anti-mouse HRP-linked antibody (Millipore, AP124P) or goat anti-rabbit HRP-linked antibody (Cell Signaling Technology, 7074), the complexes on the blot were visualized using the SuperSignal™ West Pico Chemiluminescent Substrate (Thermo Fisher Scientific, 34080) following the manufacturer's instructions.

MDC staining

To visualize the accumulation of autophagosomes, tomato leaves were excised and then immediately vacuum infiltrated with 100 μM MDC (Sigma-Aldrich, 30432) for 30 min, followed by 2 washes with phosphate-buffered saline (PBS; Solarbio, P1020) buffer. MDC-incorporated structures were monitored under a LSM 780 confocal microscope (Zeiss, Germany), excited by a wavelength of 405 nm and detected at 400 to 580 nm according to the method of Zhou et al.¹⁴

TEM analysis

For transmission electron microscopy, tomato leaves were excised and immediately cut into small pieces (~1 mm × 4 mm), then fixed with 2.5% glutaraldehyde in 0.1 M sodium cacodylate (PBS) buffer (pH 7.0) for 12 h in the dark. After washes with PBS buffer, the samples were fixed for 2 h in 1% (v/v) osmium tetroxide at room temperature; then, the samples were dehydrated in a graded ethanol series (30 to 100%; v/v) and embedded in Epon 812. Ultrathin sections (70 nm) were prepared on an ultramicrotome (Leica EM UC7, Germany) with a diamond knife and collected on Formvar-coated grids. The sections were examined using a H7650 transmission electron microscope (Hitachi, Japan) at an accelerating voltage of 75 kV to observe autophagosomes and autophagic bodies.^{32,64}

Recombinant protein and EMSA analysis

The tomato HsfA1a recombinant protein was prepared as previously described.⁶⁵ Briefly, the full-length *HsfA1a* CDS was amplified with the gene-specific primers: forward primer, 5'-AAGGAAAAAAGCGGCCGCATGGAGCCGAATTCTTAT-3' and reverse primer, 5'-CCGCTCGAGTTAGATCA-TATGTTTTTG-3'. The PCR product was digested with NotI and XhoI and ligated into the same sites of pET-32a vector. The recombinant vector was transformed into *E. coli* strain BL21 (DE3). Expression of the recombinant proteins was induced by

isopropyl β-D-1-thiogalactopyranoside and purified according to the instructions of the Novagen pET purification system.

The probes were biotin end-labeled according to the instructions of the Biotin 3' End DNA Labeling Kit (Pierce, 89818) and annealed to double-stranded probe DNA. EMSA of the HsfA1a–DNA complexes was performed according to the instructions of the LightShift Chemiluminescent EMSA kit (Thermo Fisher Scientific, 20148).

Chromatin immunoprecipitation (ChIP)

ChIP experiments were performed according to the instructions of the EpiQuik™ Plant ChIP Kit (Epigentek, P-2014). Approximately 1 g of leaf tissue was harvested from drought stress *35S-HsfA1a*-HA and wild-type plants. Chromatin was immunoprecipitated with an HA antibody (Pierce, 26183); goat anti-mouse IgG (Millipore, AP124P) was used as the negative control. ChIP-qPCR was performed with primers specific (Table S3) for the *ATG5*, *ATG8e*, *ATG10*, *ATG13b* and *ATG18f* promoters.

Statistical analysis

At least 5 independent replicates were used for each determination. Statistical analysis of the bioassays was performed using the SPSS18 statistical package. Experimental data were analyzed with Duncan multiple range test at $P < 0.05$.

Disclosure of Potential Conflicts of Interest

No potential conflicts of interest were disclosed.

Acknowledgment

We thank Dr. Zhixiang Chen for his careful reading of the manuscript.

Funding

This work was supported by the National Natural Science Foundation of China (31430076, 31401877) and the Geological Exploration Foundation of Zhejiang Province, China (2014002–02).

Supplemental Material

Supplemental data for this article can be accessed on the publisher's website.

References

1. Shaid S, Brandts CH, Serve H, Dikic I. Ubiquitination and selective autophagy. *Cell Death Differ* 2013; 20:21-30; PMID:22722335; <http://dx.doi.org/10.1038/cdd.2012.72>
2. Hartl FU, Bracher A, Hayer-Hartl M. Molecular chaperones in protein folding and proteostasis. *Nature* 2011; 475:324-32; PMID:21776078; <http://dx.doi.org/10.1038/nature10317>
3. Mizushima N, Komatsu M. Autophagy: renovation of cells and tissues. *Cell* 2011; 147:728-41; PMID:22078875; <http://dx.doi.org/10.1016/j.cell.2011.10.026>
4. Ausubel FM. Are innate immune signaling pathways in plants and animals conserved? *Nat Immunol* 2005; 6:973-9; PMID:16177805; <http://dx.doi.org/10.1038/ni1253>
5. Suzuki N, Koussevitzky S, Mittler R, Miller G. ROS and redox signalling in the response of plants to abiotic stress. *Plant Cell Environ* 2012; 35:259-70; PMID:21486305; <http://dx.doi.org/10.1111/j.1365-3040.2011.02336.x>
6. Peleg Z, Blumwald E. Hormone balance and abiotic stress tolerance in crop plants. *Curr Opin Plant Biol* 2011; 14:290-5; PMID:21377404; <http://dx.doi.org/10.1016/j.pbi.2011.02.001>
7. Bassham DC. Plant autophagy—more than a starvation response. *Curr Opin Plant Biol* 2007; 10:587-93; PMID:17702643; <http://dx.doi.org/10.1016/j.pbi.2007.06.006>
8. Klionsky DJ, Emr SD. Autophagy as a regulated pathway of cellular degradation. *Science* 2000; 290:1717-21; PMID:11099404; <http://dx.doi.org/10.1126/science.290.5497.1717>
9. Il Kwon S, Park OK. Autophagy in Plants. *J Plant Biol* 2008; 51:313-20; <http://dx.doi.org/10.1007/BF03036132>
10. Kim SH, Kwon C, Lee JH, Chung T. Genes for plant autophagy: Functions and interactions. *Mol Cells*

- 2012; 34:413-23; PMID:22772908; <http://dx.doi.org/10.1007/s10059-012-0098-y>
11. Diaz-Troya S, Perez-Perez ME, Florencio FJ, Crespo JL. The role of TOR in autophagy regulation from yeast to plants and mammals. *Autophagy* 2008; 4:851-65; PMID:18670193; <http://dx.doi.org/10.4161/autophagy.6555>
 12. Liu YM, Bassham DC. TOR is a negative regulator of autophagy in *Arabidopsis thaliana*. *Plos One* 2010; 5(7): e11883; <http://dx.doi.org/10.1371/journal.pone.0011883>
 13. Liu YM, Xiong Y, Bassham DC. Autophagy is required for tolerance of drought and salt stress in plants. *Autophagy* 2009; 5:954-63; PMID:19587533; <http://dx.doi.org/10.4161/autophagy.5.7.9290>
 14. Zhou J, Wang J, Yu JQ, Chen Z. Role and regulation of autophagy in heat stress responses of tomato plants. *Front Plant Sci* 2014; 5:174; PMID:24817875
 15. Akerfelt M, Morimoto RI, Sistonen L. Heat shock factors: integrators of cell stress, development and lifespan. *Nat Rev Mol Cell Bio* 2010; 11:545-55; <http://dx.doi.org/10.1038/nrm2938>
 16. von Koskull-Doring P, Scharf KD, Nover L. The diversity of plant heat stress transcription factors. *Trends Plant Sci* 2007; 12:452-7; PMID:17826296; <http://dx.doi.org/10.1016/j.tplants.2007.08.014>
 17. Scharf KD, Berberich T, Ebersberger I, Nover L. The plant heat stress transcription factor (Hsf) family: Structure, function and evolution. *Bba-Gene Regul Mech* 2012; 1819:104-19.
 18. Nover L, Bharti K, Doring P, Mishra SK, Ganguli A, Scharf KD. *Arabidopsis* and the heat stress transcription factor world: how many heat stress transcription factors do we need? *Cell Stress Chaperon* 2001; 6:177-89; [http://dx.doi.org/10.1038/1466-1268\(2001\)006%3c0177::AATHST%3e2.0.CO;2](http://dx.doi.org/10.1038/1466-1268(2001)006%3c0177::AATHST%3e2.0.CO;2)
 19. Kotak S, Port M, Ganguli A, Bicker F, von Koskull-Doring P. Characterization of C-terminal domains of *Arabidopsis* heat stress transcription factors (Hsfs) and identification of a new signature combination of plant class A Hsfs with AHA and NES motifs essential for activator function and intracellular localization. *Plant J* 2004; 39:98-112; PMID:15200645; <http://dx.doi.org/10.1111/j.1365-313X.2004.02111.x>
 20. Yoshida T, Ohama N, Nakajima J, Kidokoro S, Mizoi J, Nakashima K, Maruyama K, Kim JM, Seki M, Todaka D, et al. *Arabidopsis* HsfA1 transcription factors function as the main positive regulators in heat shock-responsive gene expression. *Mol Genet Genomics* 2011; 286:321-32; PMID:21931939; <http://dx.doi.org/10.1007/s00438-011-0647-7>
 21. Nishizawa-Yokoi A, Nosaka R, Hayashi H, Tainaka H, Maruta T, Tamoi M, Ikeda M, Ohme-Takagi M, Yoshimura K, Yabuta Y, et al. *Arabidopsis* HsfA1e involved in the transcriptional regulation of HsfA2 function as key regulators for the Hsf signaling network in response to environmental stress. *Plant Cell Physiol* 2011; 52:933-45; PMID:21471117; <http://dx.doi.org/10.1093/pcp/pcr045>
 22. Liu HC, Liao HT, Charng YY. The role of class A1 heat shock factors (HsfA1s) in response to heat and other stresses in *Arabidopsis*. *Plant Cell Environ* 2011; 34:738-51; PMID:21241330; <http://dx.doi.org/10.1111/j.1365-3040.2011.02278.x>
 23. Scharf KD, Heider H, Hohfeld I, Lyck R, Schmidt E, Nover L. The tomato Hsf system: HsfA2 needs interaction with HsfA1 for efficient nuclear import and may be localized in cytoplasmic heat stress granules. *Mol Cell Biol* 1998; 18:2240-51; PMID:9528795
 24. Liu Y, Zhang C, Chen J, Guo L, Li X, Li W, Yu Z, Deng J, Zhang P, Zhang K, et al. *Arabidopsis* heat shock factor HsfA1a directly senses heat stress, pH changes, and hydrogen peroxide via the engagement of redox state. *Plant Physiol Biochem* 2013; 64:92-8; PMID:23399534; <http://dx.doi.org/10.1016/j.plaphy.2012.12.013>
 25. Hahn A, Bublak D, Schleiff E, Scharf KD. Crosstalk between Hsp90 and Hsp70 Chaperones and Heat Stress Transcription Factors in Tomato. *Plant Cell* 2011; 23:741-55; PMID:21307284; <http://dx.doi.org/10.1105/tpc.110.076018>
 26. Mishra SK, Tripp J, Winkelhaus S, Tschiersch B, Theres K, Nover L, Scharf KD. In the complex family of heat stress transcription factors, HsfA1 has a unique role as master regulator of thermotolerance in tomato. *Gene Dev* 2002; 16:1555-67; PMID:12080093; <http://dx.doi.org/10.1101/gad.228802>
 27. Lee JH, Hubel A, Schoff F. Derepression of the Activity of Genetically-Engineered Heat-Shock Factor Causes Constitutive Synthesis of Heat-Shock Proteins and Increased Thermotolerance in Transgenic *Arabidopsis*. *Plant J* 1995; 8:603-12; PMID:7496404; <http://dx.doi.org/10.1046/j.1365-313X.1995.8040603.x>
 28. Turnage MA, Muangsan N, Peele CG, Robertson D. Geminivirus-based vectors for gene silencing in *Arabidopsis*. *Plant J* 2002; 30:107-14; PMID:11967097; <http://dx.doi.org/10.1046/j.1365-313X.2002.01261.x>
 29. Brigneti G, Martin-Hernandez AM, Jin HL, Chen J, Baulcombe DC, Baker B, Jones JD. Virus-induced gene silencing in Solanum species. *Plant J* 2004; 39:264-72; PMID:15225290; <http://dx.doi.org/10.1111/j.1365-313X.2004.02122.x>
 30. Liu YL, Schiff M, Dinesh-Kumar SP. Virus-induced gene silencing in tomato. *Plant J* 2002; 31:777-86; PMID:12220268; <http://dx.doi.org/10.1046/j.1365-313X.2002.01394.x>
 31. Zhou J, Wang J, Cheng Y, Chi YJ, Fan B, Yu JQ, Chen Z. NBR1-mediated selective autophagy targets insoluble ubiquitinated protein aggregates in plant stress responses. *PLoS Genet* 2013; 9:e1003196; PMID:23341779; <http://dx.doi.org/10.1371/journal.pgen.1003196>
 32. Wang Y, Yu B, Zhao J, Guo J, Li Y, Han S, Huang L, Du Y, Hong Y, Tang D, et al. Autophagy contributes to leaf starch degradation. *Plant Cell* 2013; 25:1383-99; PMID:23564204; <http://dx.doi.org/10.1105/tpc.112.108993>
 33. Kwon SI, Cho HJ, Kim SR, Park OK. The Rab GTPase RabG3b positively regulates autophagy and immunity-associated hypersensitive cell death in *Arabidopsis*. *Plant Physiol* 2013; 161:1722-36; PMID:23404918; <http://dx.doi.org/10.1104/pp.112.208108>
 34. Lobell DB, Burke MB, Tebaldi C, Mastrandrea MD, Falcon WP, Naylor RL. Prioritizing climate change adaptation needs for food security in 2030. *Science* 2008; 319:607-10; PMID:18239122; <http://dx.doi.org/10.1126/science.1152339>
 35. Zhu JK. Salt and drought stress signal transduction in plants. *Annu Rev Plant Biol* 2002; 53:247-73; PMID:12221975; <http://dx.doi.org/10.1146/annurev.arplant.53.091401.143329>
 36. Yamaguchi-Shinozaki K, Shinozaki K. Transcriptional regulatory networks in cellular responses and tolerance to dehydration and cold stresses. *Annu Rev Plant Biol* 2006; 57:781-803; PMID:16669782; <http://dx.doi.org/10.1146/annurev.arplant.57.032905.105444>
 37. Shinozaki K, Yamaguchi-Shinozaki K. Gene networks involved in drought stress response and tolerance. *J Exp Bot* 2007; 58:221-7; PMID:17075077; <http://dx.doi.org/10.1093/jxb/erl164>
 38. Hoekstra FA, Golovina EA, Buitink J. Mechanisms of plant desiccation tolerance. *Trends Plant Sci* 2001; 6:431-8; PMID:11544133; [http://dx.doi.org/10.1016/S1360-1385\(01\)02052-0](http://dx.doi.org/10.1016/S1360-1385(01)02052-0)
 39. Vinocur B, Altman A. Recent advances in engineering plant tolerance to abiotic stress: achievements and limitations. *Curr Opin Biotech* 2005; 16:123-32; PMID:15831376; <http://dx.doi.org/10.1016/j.copbio.2005.02.001>
 40. Goyal K, Walton LJ, Tunnacliffe A. LEA proteins prevent protein aggregation due to water stress. *Biochem J* 2005; 388:151-7; PMID:15631617; <http://dx.doi.org/10.1042/BJ20041931>
 41. Wang WX, Vinocur B, Shoseyov O, Altman A. Role of plant heat-shock proteins and molecular chaperones in the abiotic stress response. *Trends Plant Sci* 2004; 9:244-52; PMID:15130550; <http://dx.doi.org/10.1016/j.tplants.2004.03.006>
 42. Liu LJ, Cui F, Li QL, Yin BJ, Zhang HW, Lin BY, Wu Y, Xia R, Tang S, Xie Q. The endoplasmic reticulum-associated degradation is necessary for plant salt tolerance. *Cell Res* 2011; 21:957-69; PMID:21187857; <http://dx.doi.org/10.1038/cr.2010.181>
 43. Zhou J, Zhang Y, Qi JX, Chi YJ, Fan BF, Yu JQ, et al. E3 ubiquitin ligase CHIP and NBR1-mediated selective autophagy protect additively against proteotoxicity in plant stress responses. *PLoS Genet* 2014; 10(1): e1004116; <http://dx.doi.org/10.1371/journal.pgen.1004116>
 44. Kraft E, Stone SL, Ma LG, Su N, Gao Y, Lau OS, Deng XW, Callis J. Genome analysis and functional characterization of the E2 and RING-type E3 ligase ubiquitination enzymes of *Arabidopsis*. *Plant Physiol* 2005; 139:1597-611; PMID:16339806; <http://dx.doi.org/10.1104/pp.105.067983>
 45. Walsh CK, Sadanandom A. Ubiquitin chain topology in plant cell signaling: a new facet to an evergreen story. *Front Plant Sci* 2014; 5:122; <http://dx.doi.org/10.3389/fpls.2014.00122>
 46. Gamberdinger M, Carra S, Behl C. Emerging roles of molecular chaperones and co-chaperones in selective autophagy: focus on BAG proteins. *J Mol Med* 2011; 89:1175-82; PMID:21818581; <http://dx.doi.org/10.1007/s00109-011-0795-6>
 47. Kim YE, Hipp MS, Bracher A, Hayer-Hardt M, Hardt FU. Molecular Chaperone Functions in Protein Folding and Proteostasis. *Annu Rev Biochem* 2013; 82:323-55; PMID:23746257; <http://dx.doi.org/10.1146/annurev-biochem-060208-092442>
 48. Dokladny K, Myers OB, Moseley PL. Heat shock response and autophagy—cooperation and control. *Autophagy* 2015; 11:200-13; PMID:25714619; <http://dx.doi.org/10.1080/15548627.2015.1009776>
 49. Bence NF, Sampat RM, Kopito RR. Impairment of the ubiquitin-proteasome system by protein aggregation. *Science* 2001; 292:1552-5; PMID:11375494; <http://dx.doi.org/10.1126/science.292.5521.1552>
 50. Peteranderl R, Rabenstein M, Shin YK, Liu CW, Wemmer DE, King DS, Nelson HC. Biochemical and biophysical characterization of the trimerization domain from the heat shock transcription factor. *Biochem* 1999; 38:3559-69; <http://dx.doi.org/10.1021/bi981774j>
 51. Busch W, Wunderlich M, Schoff F. Identification of novel heat shock factor-dependent genes and biochemical pathways in *Arabidopsis thaliana*. *Plant J* 2005; 41:1-14; PMID:15610345; <http://dx.doi.org/10.1111/j.1365-313X.2004.02272.x>
 52. Phillips AR, Suttangkakul A, Vierstra RD. The ATG12-conjugating enzyme ATG10 is essential for autophagic vesicle formation in *Arabidopsis thaliana*. *Genetics* 2008; 178:1339-53; PMID:18245858; <http://dx.doi.org/10.1534/genetics.107.086199>
 53. Xiong Y, Contento AL, Bassham DC. AtATG18a is required for the formation of autophagosomes during nutrient stress and senescence in *Arabidopsis thaliana*. *Plant J* 2005; 42:535-46; PMID:15860012; <http://dx.doi.org/10.1111/j.1365-313X.2005.02397.x>
 54. Rizhsky L, Liang HJ, Shuman J, Shulaev V, Davletova S, Mittler R. When defense pathways collide. The response of *Arabidopsis* to a combination of drought and heat stress. *Plant Physiol* 2004; 134:1683-96; PMID:15047901; <http://dx.doi.org/10.1104/pp.103.033431>
 55. Desai S, Liu ZX, Yao J, Patel N, Chen JQ, Wu Y, Ahn EE, Fodstad O, Tan M. Heat shock factor 1 (HSF1) controls chemoresistance and autophagy through transcriptional regulation of autophagy-related protein 7 (ATG7). *J Biol Chem* 2013; 288:9165-76; PMID:23386620; <http://dx.doi.org/10.1074/jbc.M112.422071>
 56. Chan-Schaminet KY, Baniwal SK, Bublak D, Nover L, Scharf KD. Specific interaction between tomato HsfA1 and HsfA2 creates hetero-oligomeric superactivator complexes for synergistic activation of heat stress gene expression. *J Biol Chem* 2009; 284:20848-57;

- PMID:19491106; <http://dx.doi.org/10.1074/jbc.M109.007336>
57. Li SX, Liu JX, Liu ZY, Li XR, Wu FJ, He YK. *HEAT-INDUCED TAS1 TARGET1* mediates thermotolerance via HEAT STRESS TRANSCRIPTION FACTOR A1a-directed pathways in *Arabidopsis*. *Plant Cell* 2014; 26:1764-80; PMID:24728648; <http://dx.doi.org/10.1105/tpc.114.124883>
 58. Fillatti JJ, Kiser J, Rose R, Comai L. Efficient transfer of a glyphosate tolerance gene into tomato using a binary *Agrobacterium tumefaciens* vector. *Bio-Technol* 1987; 5:726-30; <http://dx.doi.org/10.1038/nbt0787-726>
 59. Ekengren SK, Liu YL, Schiff M, Dinesh-Kumar SP, Martin GB. Two MAPK cascades, NPR1, and TGA transcription factors play a role in Pto-mediated disease resistance in tomato. *Plant J* 2003; 36:905-17; PMID:14675454; <http://dx.doi.org/10.1046/j.1365-313X.2003.01944.x>
 60. Xia XJ, Gao CJ, Song LX, Zhou YH, Shi K, Yu JQ. Role of H₂O₂ dynamics in brassinosteroid-induced stomatal closure and opening in *Solanum lycopersicum*. *Plant Cell Environ* 2014; 37:2036-50; PMID:24428600; <http://dx.doi.org/10.1111/pce.12275>
 61. Zhou YH, Lam HM, Zhang JH. Inhibition of photosynthesis and energy dissipation induced by water and high light stresses in rice. *J Exp Bot* 2011; 58:1207-17; <http://dx.doi.org/10.1093/jxb/erl291>
 62. Welsch R, Wust F, Bar C, Al-Babili S, Beyer P. A third phytoene synthase is devoted to abiotic stress-induced abscisic acid formation in rice and defines functional diversification of phytoene synthase genes. *Plant Physiol* 2008; 147:367-80; PMID:18326788; <http://dx.doi.org/10.1104/pp.108.117028>
 63. Livak KJ, Schmittgen TD. Analysis of relative gene expression data using real-time quantitative PCR and the 2(-Delta Delta C) method. *Methods* 2001; 25:402-8; PMID:11846609; <http://dx.doi.org/10.1006/meth.2001.1262>
 64. Yoshimoto K, Hanaoka H, Sato S, Kato T, Tabata S, Noda T, Ohsumi Y. Processing of ATG8s, ubiquitin-like proteins, and their deconjugation by ATG4s are essential for plant autophagy. *Plant Cell* 2004; 16:2967-83; PMID:15494556; <http://dx.doi.org/10.1105/tpc.104.025395>
 65. Lai ZB, Li Y, Wang F, Cheng Y, Fan BF, Yu JQ, Chen Z. *Arabidopsis* sigma factor binding proteins are activators of the WRKY33 transcription factor in plant defense. *Plant Cell* 2011; 23:3824-41; PMID:21990940; <http://dx.doi.org/10.1105/tpc.111.090571>